Article

Cell Metabolism

Inhibition of Intracellular Triglyceride Lipolysis Suppresses Cold-Induced Brown Adipose Tissue Metabolism and Increases Shivering in Humans

Graphical Abstract

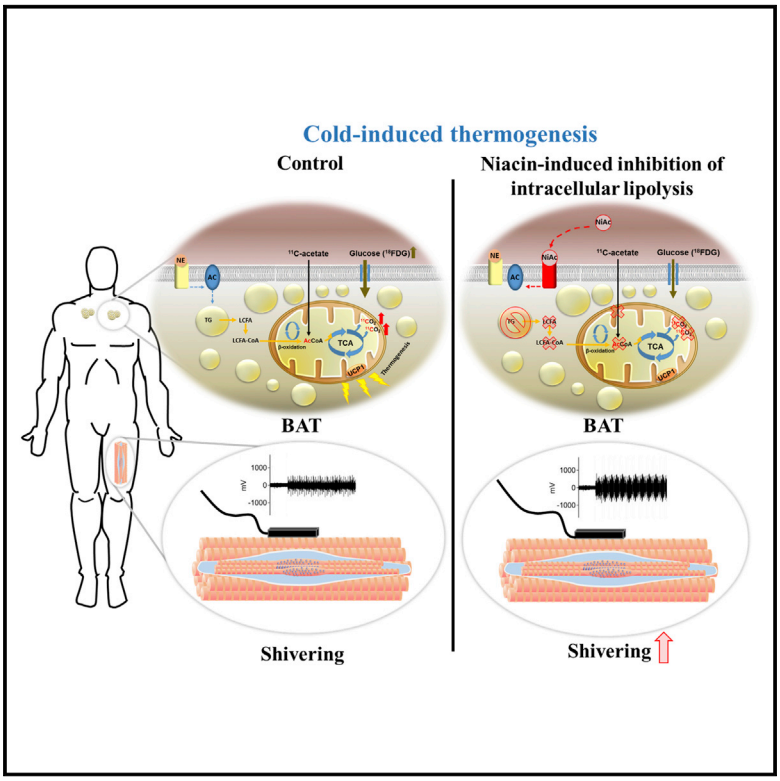

Authors

Denis P. Blondin, Frédérique Frisch, Serge Phoenix, ..., François Haman, Denis Richard, André C. Carpentier

Correspondence

andre.carpentier@usherbrooke.ca

In Brief

Blondin et al. use PET imaging in humans to demonstrate that brown adipose tissue uses lipids as its cellular fuel source for thermogenesis. Inhibition of intracellular TG lipolysis resulted in suppressed BAT thermogenesis, which was offset by an increase in shivering intensity.

Highlights

- Niacin-induced inhibition of lipolysis abolishes mobilization of lipids in BAT
- Inhibition of adipose tissue lipolysis abolishes cold-induced BAT thermogenesis
- Inhibition of BAT lipolysis did not abolish cold-stimulated BAT perfusion
- Inhibiting BAT thermogenesis was compensated by commensurate increase in shivering

Blondin et al., 2017, Cell Metabolism *25*, 438–447
February 7, 2017
http://dx.doi.org/10.1016/j.cmet.2016.12.005

CellPress

Cell Metabolism
Article

Inhibition of Intracellular Triglyceride Lipolysis Suppresses Cold-Induced Brown Adipose Tissue Metabolism and Increases Shivering in Humans

Denis P. Blondin,[1] Frédérique Frisch,[1] Serge Phoenix,[1,4] Brigitte Guérin,[4] Éric E. Turcotte,[4] François Haman,[3] Denis Richard,[2] and André C. Carpentier[1,5,*]

[1]Department of Medicine, Centre de Recherche du Centre Hospitalier Universitaire de Sherbrooke, Université de Sherbrooke, Sherbrooke, QC J1K 2R1, Canada

[2]Centre de Recherche de l'Institut Universitaire de Cardiologie et de Pneumologie de Québec, Université Laval, QC G1V 4G5, Canada

[3]Faculty of Health Sciences, University of Ottawa, Ottawa, ON K1N 6N5, Canada

[4]Department of Nuclear Medicine and Radiobiology, Centre d'Imagerie Moléculaire de Sherbrooke, Université de Sherbrooke, Sherbrooke, QC J1K 2R1, Canada

[5]Lead Contact

*Correspondence: andre.carpentier@usherbrooke.ca

http://dx.doi.org/10.1016/j.cmet.2016.12.005

SUMMARY

Indirect evidence from human studies suggests that brown adipose tissue (BAT) thermogenesis is fueled predominantly by fatty acids hydrolyzed from intracellular triglycerides (TGs). However, no direct experimental evidence to support this assumption currently exists in humans. The aim of this study was to determine the role of intracellular TG in BAT thermogenesis, in cold-exposed men. Using positron emission tomography with ^{11}C-acetate and ^{18}F-fluorodeoxyglucose, we showed that oral nicotinic acid (NiAc) administration, an inhibitor of intracellular TG lipolysis, suppressed the cold-induced increase in BAT oxidative metabolism and glucose uptake, despite no difference in BAT blood flow. There was a commensurate increase in shivering intensity and shift toward a greater reliance on glycolytic muscle fibers without modifying total heat production. Together, these findings show that intracellular TG lipolysis is critical for BAT thermogenesis and provides experimental evidence for a reciprocal role of BAT thermogenesis and shivering in cold-induced thermogenesis in humans.

INTRODUCTION

The sympathetic nervous system (SNS) stimulates white adipose tissue (WAT) fatty acid mobilization via the hydrolysis of intracellular triglycerides (TG) (Bartness et al., 2014). Resistance to catecholamine action on WAT appears to be an important feature of obesity and insulin resistance (Horowitz et al., 1999; Jocken et al., 2007, 2008) and may potentially extend to other important adipose depots, such as brown adipose tissue (BAT). This, in turn, could result in a blunted thermogenic response and energy dissipating potential since the fatty acids released from catecholamine-mediated lipolysis serve as both activators and metabolic substrates fueling BAT thermogenesis (Fedorenko et al., 2012). What remains unclear is the extent to which intracellular TG are critical for BAT thermogenesis in humans and whether circulating substrates can contribute substantially to fueling this thermogenesis.

The SNS stimulation resulting from mild cold exposure leads to a 2-fold increase in BAT oxidative metabolism in lean healthy and overweight men with and without well-controlled type 2 diabetes (T2D) (Blondin et al., 2015a, 2015b). This increase in BAT thermogenesis is supported in small part by circulating glucose (Blondin et al., 2014a, 2015a, 2015b; Cypess et al., 2012; Hanssen et al., 2015; Muzik et al., 2012; Orava et al., 2011; Ouellet et al., 2012) and fatty acids mobilized from WAT (Blondin et al., 2015a; Ouellet et al., 2012). The rapid increase in BAT radio-density during acute cold exposure led to the assumption that BAT thermogenesis is fueled predominantly by fatty acids hydrolyzed from intracellular TG (Baba et al., 2010; Blondin et al., 2015a, 2015b; Ouellet et al., 2012). Rats acutely and chronically exposed to the cold (10°C), given nicotinic acid (NiAc), an inhibitor of intracellular TG lipolysis, show a suppression in interscapular BAT oxidative metabolism and uptake of both circulating glucose and fatty acids (Labbé et al., 2015). This demonstrates that, in rodents, fatty acids derived from intracellular TG are essential for BAT thermogenesis. Whether intracellular TG are as critical for human BAT thermogenesis and whether circulating glucose can directly serve as a substrate to fuel BAT thermogenesis remains unclear, but may explain the diminished whole-body BAT thermogenesis and greater lipid content seen in older overweight men with or without T2D (Blondin et al., 2015a). In the present study, we used positron emission tomography (PET) with ^{11}C-acetate and ^{18}F-fluorodeoxyglucose (^{18}FDG) to determine the role of intracellular TG and circulating glucose on BAT oxidative metabolism, in cold-exposed men. We hypothesized that NiAc administration would blunt cold-stimulated BAT oxidative metabolism, while abolishing cold-induced intracellular brown adipocyte TG lipolysis.

RESULTS

There were eight healthy, non-cold acclimatized men aged 30 years (95% confidence interval [CI]: 25 to 35) with a BMI of

Table 1. Hormone and Metabolite Concentrations at Room Temperature and Cold Exposure without and with the Ingestion of Nicotinic Acid

	Control[a]		NiAc		p values		
	Room Temperature	Cold Exposure	Room Temperature	Cold Exposure	Temp.	NiAc	T × C
T_{skin}[b] (°C)	33.6 (33.2 – 34.0)	27.7 (27.1 – 28.2)	33.7 (33.2 – 34.3)	28.2 (27.5 – 28.9)	<0.0001	0.17	0.04
T_{core} (°C)	36.8 (36.6 – 36.9)	36.5 (36.2 – 36.9)	36.8 (36.6 – 37.0)	36.5 (36.1 – 36.9)	0.04	0.87	0.55
$\Delta T_{inlet\text{-}outlet}$ of suit (°C)[c]	–	2.6 [2.5 – 2.7]	–	2.8 [2.6 – 3.0]	–	0.14	–
EE ($kJ.min^{-1}$)‡	4.9 (4.5 – 5.4)	8.2 (6.7 – 9.8)	4.8 (4.1 – 5.5)	8.4 (6.3 – 10.6)	0.0006	0.93	0.59
Ox_{CHO} ($\mu mol.min^{-1}$)[c]	670 (573 – 767)	895 (560 – 1230)	593 (428 – 759)	1,303 (1,083 – 1,522)	0.002	0.06	0.02
$Ra_{glucose}$ ($\mu mol.min^{-1}$)	1,718 (1,498 – 1,937)	1,182 (1,051 – 1,312)	1,710 (1,326 – 2,094)	1,404 (1,121 – 1,688)	0.0007	0.26	0.02
Glucose (mmol/L)	4.7 (4.3 – 5.1)	4.5 (4.2 – 4.8)	4.8 (4.5 – 5.1)	4.7 (4.5 – 5.0)	0.10	0.06	0.30
Insulin (pmol/L)	26.5 [22.2 – 72.3]	25.7 [13.2 – 52.2]	31.2 [20.6 – 60.5]	25.1 [18.9 – 35.8]	0.02	0.80	0.44
Glucagon (pg/mL)	26.2 [24.6 – 34.8]	26.0 [22.9 – 29.2]	26.9 [18.2 – 40.6]	40.2 [36.7 – 47.5]	0.02	0.07	0.005
TG (mmol/L)	1.1 [0.5 – 1.2]	1.1 [0.6 – 1.2]	0.8 [0.5 – 1.2]	0.8 [0.5 – 1.0]	0.54	0.05	0.06
NEFA (μmol/L)	285 [200 – 323]	442 [407 – 595]	295 [193 – 453]	157 [71 – 179]	0.30	0.003	0.0001
TSH (IU/L)	2.2 [1.6 – 2.8]	1.9 [1.4 – 2.6]	2.1 [1.5 – 2.3]	1.8 [1.5 – 2.1]	0.004	0.75	0.30
Free T3 (pmol/L)	5.5 [5.0 – 6.1]	5.4 [4.9 – 5.6]	5.5 [4.7 – 5.9]	5.5 [4.7 – 5.9]	0.23	0.63	0.33
Free T4 (pmol/L)	15.3 (13.0 – 17.6)	16.9 (15.1 – 18.7)	16.6 (15.1 – 18.2)	17.3 (15.7 – 18.9)	0.02	0.08	0.31
Cortisol (nmol/L)	328 (252 – 405)	293 (240 – 347)	360 (314 – 407)	455 (368 – 542)	0.10	0.004	0.03
Leptin (ng/mL)	2.2 (0.6 – 3.9)	1.7 (0.2 – 3.1)	2.4 (1.1 – 3.6)	1.7 (0.6 – 2.8)	0.0007	0.66	0.44
Ghrelin (ng/L)	502 (418 – 586)	554 (452 – 657)	495 (401 – 590)	362 (304 – 420)	0.04	0.0001	0.001
Adiponectin (μg/mL)	6.7 (5.3 – 8.2)	5.5 (4.4 – 6.6)	6.4 (5.4 – 7.5)	5.5 (4.5 – 6.5)	0.001	0.39	0.23

[a]Values are means with 95% CI in parentheses for normally distributed data and median [interquartile range] for non-parametric data. Temp. refers to an effect of temperature, NiAc an effect of nicotinic acid ingestion, and T x C the interaction between temperature and nicotinic acid ingestion determined using repeated-measures two-way ANOVA with Bonferonni post-hoc test.

[b]T_{skin}, mean skin temperature; T_{core}, core temperature; $\Delta T_{inlet\text{-}outlet}$ of suit, change in inlet-outlet suit water temperature; EE, energy expenditure; Ox_{CHO}, rate of whole-body carbohydrate oxidation; Ra, appearance rate; TG; and NEFA.

[c]n = 7.

24.5 kg/m^2 (95% CI: 22.3 to 26.6) that participated in the present study protocol. During cold exposure, the mean skin temperature fell by 6.0°C (95% CI: 5.4 to 6.6) in the control condition and 5.6°C (95% CI: 4.6 to 6.6) when given NiAc (p = 0.41) and core temperature decreased marginally (Table 1). This resulted in a ~1.7-fold increase in energy expenditure (ΔEE of 3.3 $kJ.min^{-1}$ [95% CI: 1.8 to 4.7] in control and 3.6 $kJ.min^{-1}$ (95% CI: 2.0 to 5.2) with NiAc; Table 1). Metabolite and hormone levels are presented in Table 1. NiAc resulted in the expected reduction in plasma non-esterified fatty acid (NEFA) levels versus increased levels in control (interaction NiAc × temperature $p < 0.01$). NiAc administration also led to greater cold-stimulated increase in carbohydrate oxidation (CHO_{ox}), glucagon and cortisol, and lower cold-induced reduction in glucose appearance rate ($Ra_{glucose}$) (all interaction NiAc × temperature $p < 0.05$).

Inhibition of Intracellular Lipolysis

Cold exposure evoked a 1.4-fold increase in Ra_{NEFA} during cold exposure (Figure 1A) and a 2.2-fold increase in $Ra_{glycerol}$ (Figure 1B). The oral ingestion of NiAc suppressed Ra_{NEFA} and $Ra_{glycerol}$ during cold exposure by 50% (95% CI: 22 to 78) and 55% (95% CI: 25 to 85), respectively (interaction NiAc × temperature, $p < 0.05$). The radio-density of BAT during the control condition, an indicator of intracellular TG content, increased during cold exposure, whereas it remained unchanged when given NiAc (interaction NiAc × temperature, p = 0.003) (Figure 1C). Fatty acid oxidation increased 1.7-fold during cold exposure in the control condition (95% CI: 1.0 to 2.4) and similarly by 1.8-fold when given NiAc (95% CI: 1.1 to 2.4) (effect of time, p = 0.01) (Figure 1D).

BAT Oxidative Metabolism and Blood Flow

Aortic arch and supraclavicular BAT ^{11}C radioactivity over time at room temperature and during cold exposure with and without NiAc are shown in Figures 2A–2D. In response to cold exposure, BAT oxidative metabolism increased 4.4-fold from 0.007 s^{-1} (95% CI: 0.002 to 0.014) at room temperature to 0.031 s^{-1} (95% CI: 0.015 to 0.057) during cold exposure. NiAc suppressed the cold-induced increase in oxidative metabolism in supraclavicular BAT by 71% (95% CI: 33 to 109) (interaction NiAc × temperature, p = 0.05) (Figure 2E). The peak BAT ^{11}C radioactivity, an index of tissue perfusion (Tadamura et al., 1996), increased as a result of cold exposure, but was not altered as a result of the ingestion of NiAc (Figure 2F).

Organ-Specific Glucose Uptake and Partitioning

The relative bio-distribution of ^{18}FDG during cold exposure without and with the ingestion of NiAc is shown in Figure 3A. The fractional glucose uptake of BAT was significantly greater than the average of muscles in the cervicothoracic region and the cervical subcutaneous white adipose tissue (Figure 3B) (two-way ANOVA interaction tissue × temperature, p = 0.01). The fractional glucose uptake in BAT was suppressed on average by 38% (95% CI: 12 to 65) when given NiAc

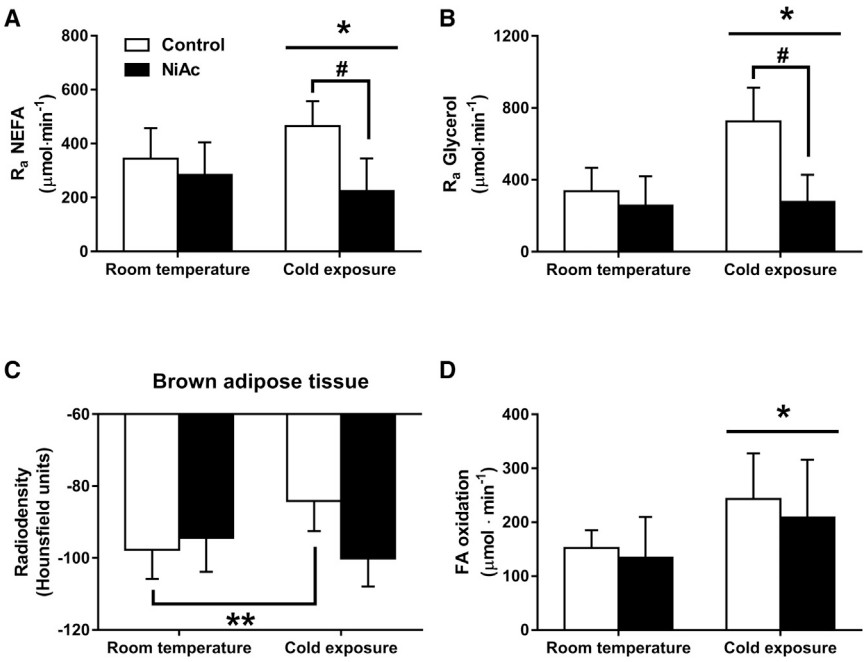

Figure 1. Lipolytic Response

(A–D) Appearance rate of NEFA (R_a NEFA) (A) and Glycerol (R_a Glycerol) (B) at room temperature and during cold exposure under control condition and following the ingestion of NiAc. The radiodensity of BAT at room temperature and during cold exposure under control condition and following the ingestion of NiAc (C) is shown. Whole-body fatty acid oxidation (D) at room temperature and during cold exposure under control condition and following the ingestion of NiAc is shown. The data are reported as the mean with 95% CI. Different from room temperature at $^{*}p < 0.05$ and $^{**}p < 0.01$; different from control at $^{\#}p < 0.05$, and two-way ANOVA with Bonferonni post-hoc test.

(p = 0.02). Similarly, the net glucose uptake of BAT was significantly greater than the average of muscles in the cervicothoracic region and the cervical subcutaneous white adipose tissue (Figure 3C) (two-way ANOVA interaction tissue × temperature, p = 0.01). The net glucose uptake in BAT was suppressed on average by 35% (95% CI: 9 to 62) when given NiAc (p = 0.03). Total glucose uptake during cold exposure was significantly greater in skeletal muscle compared to BAT (Figure 3D), accounting for 46% (95% CI: 35 to 56) of glucose turnover in muscle compared to 0.2% (95% CI: 0.04 to 0.4) in BAT (Figure 3E). When examining the bio-distribution of ^{18}FDG, glucose uptake was the highest in the myocardium (Figure 3F). The ingestion of NiAc reduced the uptake of glucose in BAT (p = 0.003), but increased glucose uptake in the myocardium (p = 0.01). There was also an association between the net glucose uptake and shivering intensity in m. pectoralis major (r = 0.62, p < 0.01; Figure 3G) and across all muscles measured by EMG (r = 0.60, p < 0.0001).

Shivering Response

Surface electromyography was used to examine the effects of ingesting NiAc on the shivering intensity and pattern (continuous versus burst shivering; Haman et al., 2004a) of eight muscles. Shivering intensity increased by a median of 149% (interquartile range [IQR]: 12% to 224%) when given NiAc (p = 0.05) (Figure 4A). This increased shivering intensity could be accounted for by a greater shivering intensity from burst shivering (p = 0.04) (Figure 4D). The shivering burst rate when given NiAc was associated with skeletal muscle glucose uptake (r = 0.72, p = 0.04) (Figure 4E) and with whole-body carbohydrate oxidation rate (r = 0.78, p = 0.04) (Figure 4F).

DISCUSSION

Experimental studies in rodent models have suggested that hydrolysis of intracellular lipids and oxidation of long-chain fatty acids are important for BAT thermogenesis (Haemmerle et al., 2006; Labbé et al., 2015; Lee et al., 2015; Osuga et al., 2000), but there were no data supporting that role in humans. The aim of the present study was to determine the role of intracellular TG lipolysis in fueling BAT thermogenesis in humans during an acute cold exposure. Our results using NiAc provide strong evidence that intracellular TG lipolysis is critical for acute cold-induced BAT oxidative metabolism in humans. NiAc administration inhibited the cold-induced increase in plasma NEFA and glycerol appearance rates, markers of WAT intracellular TG lipolysis, and the increase in BAT CT radio-density, a marker of BAT intracellular TG lipolysis. Cold-induced stimulation resulted in an increase in BAT blood flow to carry circulating substrates to the tissue, but this was insufficient to sustain BAT oxidative metabolism, which was suppressed by 71% with NiAc administration. Suppressing intracellular TG lipolysis also resulted in a commensurate increase in shivering intensity and burst shivering rate reflecting a preferential recruitment of glycolytic muscle fibers, associated with preferential increase in carbohydrate oxidation.

Cold exposure results in the stimulation of the SNS, leading to the initiation of autonomic thermoregulatory responses and adipose tissue lipolysis (Bartness et al., 2014; Morrison, 2016). Fatty acids released upon SNS-mediated hydrolysis of intracellular TG serve as both activators and metabolic substrates fueling BAT thermogenesis (Cannon and Nedergaard, 2004). To date, human studies have shown that although circulating glucose and fatty acids are taken up by stimulated BAT, representing ~1% and ~0.25% of plasma glucose and NEFA turnover, respectively (Blondin et al., 2014a, 2015a, 2015b; Din et al., 2016; Ouellet et al., 2012), a rapid increase in BAT radio-density suggests that intracellular TG are the primary fuel to sustain BAT thermogenesis during acute cold exposure. Here, we provide experimental evidence in humans that inhibiting BAT intracellular TG lipolysis using NiAc significantly suppresses BAT oxidative metabolism. NiAc acts primarily on the "metabolite-sensing" G_i-protein coupled receptor GPR109A, expressed predominantly in WAT and BAT, which upon activation inhibits adenylyl cyclase and the resultant cAMP signaling cascade required for intracellular TG lipolysis (Ahmed et al.,

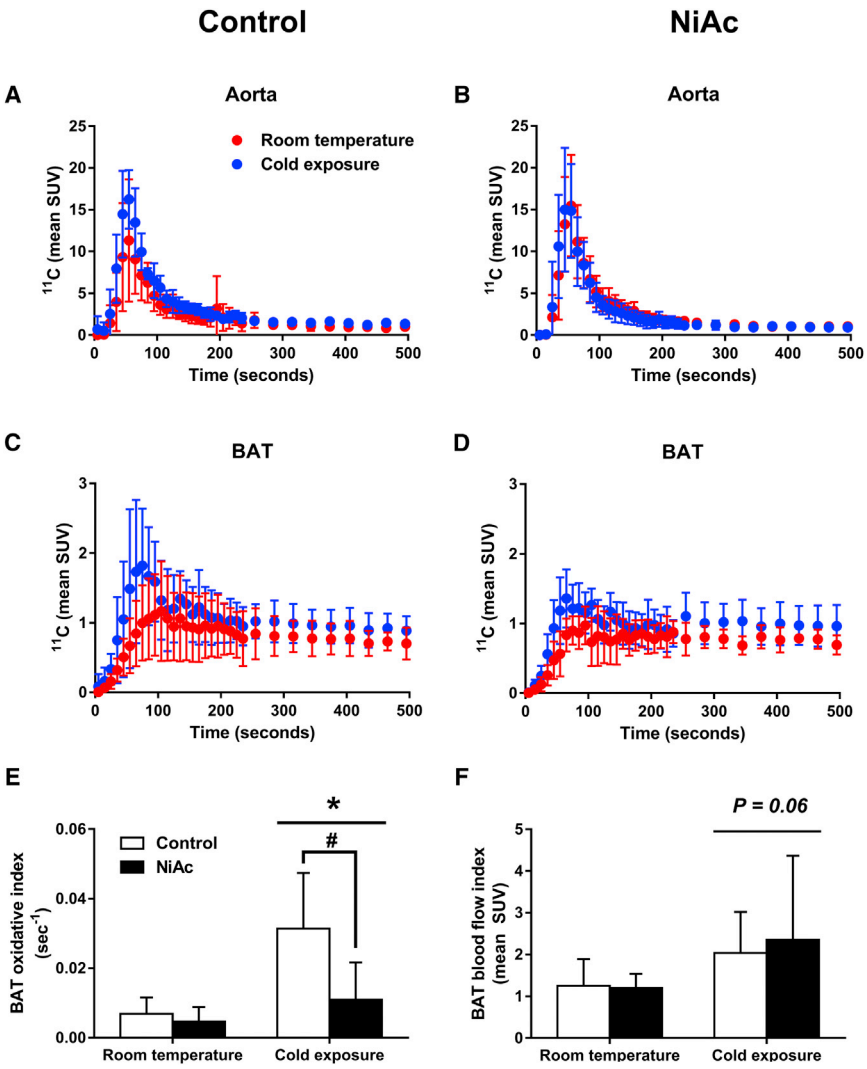

Figure 2. [^{11}C]-Acetate Kinetics

(A–F) ^{11}C time-radioactivity curves over the first 500 s of acquisition after [^{11}C]-acetate injection at room temperature and during cold exposure in aorta (A and B) and supraclavicular BAT (C and D). The monoexponential decay slope from peak tissue ^{11}C activity (BAT oxidative index) in supraclavicular BAT (E) and peak BAT ^{11}C activity in supraclavicular BAT (BAT blood flow index) (F) at room temperature and during cold exposure under control condition and following the ingestion of NiAc is shown. The data are reported as the mean with 95% CI. Different from room temperature at $^{*}p < 0.05$ and different from control at $^{\#}p < 0.05$ versus control and two-way ANOVA with Bonferonni post-hoc test.

2009). A previous study that we performed in rats also showed that NiAc suppresses the increase in oxidative metabolism in interscapular BAT by 84% during an acute cold and by 73% following more chronic cold exposure (Labbé et al., 2015). Other rodent studies have shown that mice lacking ATGL (Haemmerle et al., 2006), the rate-limiting enzyme for intracellular TG lipolysis, or an adipose-specific loss of CPT2 (Lee et al., 2015), necessary for the initiation of β-oxidation of long-chain fatty acids, show severe thermoregulatory defects. These findings combined with the present results demonstrate just how essential the hydrolysis of intracellular TG is for BAT thermogenesis. Indeed, based on [^{11}C]acetate data, we estimated that the intracellular TG pools contributed up to 71% of BAT thermogenesis during mild cold exposure. This is consistent with previous estimates from studies performed with cold-exposed rats (Labbé et al., 2015) and experiments using isolated adipocytes (Li et al., 2014). Referring to the BAT-specific metabolic rate previously reported (Din et al., 2016; Muzik et al., 2012, 2013), we can estimate that this would represent a minimum of 108 mg of intracellular BAT TG over the course of the 3 hr cold exposure.

Since the ingestion of NiAc suppressed total glucose uptake in BAT by 26% and WAT lipolytic rate by 62%, we cannot exclude the possibility that a reduction in glucose uptake and supply of circulating NEFA may have contributed to the observed reduction in BAT thermogenesis. We estimate that a total of 114 mg of glucose was taken up by BAT over the course of the 3 hr cold exposure in the control condition compared to 52 mg when given NiAc. Our data demonstrate that NiAc did not reduce systemic glucose turnover nor BAT blood flow. We acknowledge that it is impossible to determine from our in vivo study whether NiAc-induced reduction in BAT glucose uptake is solely the consequence of inhibition of intracellular lipolysis and reduced BAT oxidative metabolism, or whether other additional cellular mechanisms could have been involved. It is possible that the NiAc may have impaired β_3-adrenergic receptor-stimulated intracellular glucose transport (Olsen et al., 2014), which might explain the reduced fractional glucose extraction in the present study (Figure 3B). We and others have also previously shown a strong coupling between intracellular TG turnover and glucose uptake (Baba et al., 2010; Blondin et al., 2015a, 2015b), which suggests that glucose taken up by BAT may be necessary for replenishing TG levels. In fact, in vitro experiments in humans and in vivo studies in rodents have shown that glucose is predominantly directed toward glycerol-3-phosphate production for TG synthesis rather than oxidation (Barquissau et al., 2016; Brito et al., 1999; Himms-Hagen, 1965; Laplante et al., 2009; Moura et al., 2005).

Due to radiation exposure limits to participants, it was not possible to use the long-chain fatty acid PET tracer ^{18}FTHA in the present study. However, our previous investigation in rats showed that NiAc suppressed BAT NEFA uptake to basal/room temperature levels (Labbé et al., 2015). Assuming a similar trend here, referring to BAT NEFA uptake rates previously reported in humans at room temperature (Din et al., 2016), we

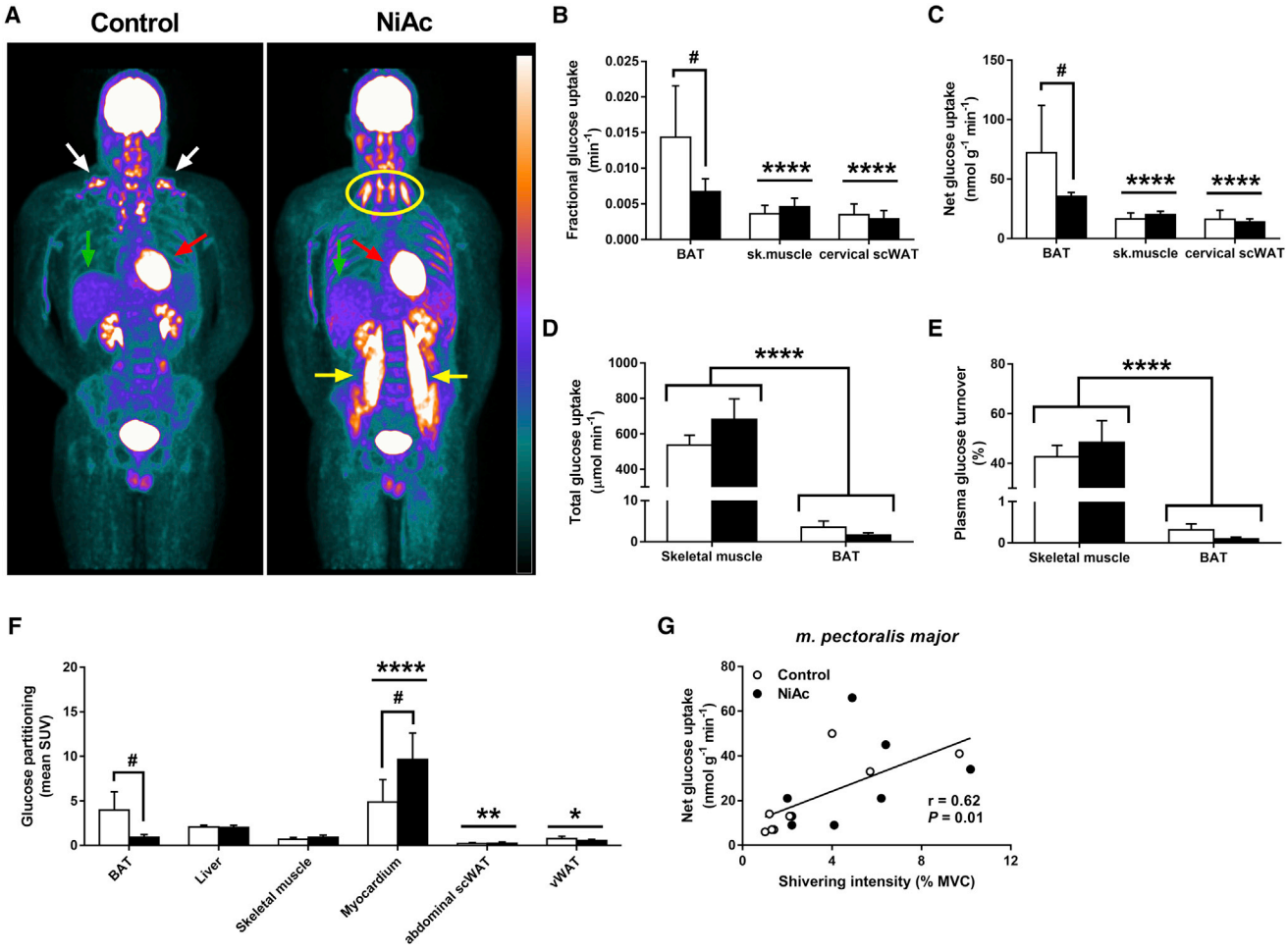

Figure 3. Tissue Glucose Uptake

(A) Coronal view (anterior-posterior projection) of whole-body ^{18}FDG uptake during cold exposure without and with oral ingestion of NiAc. The white arrows show bilateral supraclavicular BAT depots, the red arrows show myocardium, the green arrows show liver, the yellow circle shows m. sternocleidomastoideus (laterally) and m. sternothyroideus (medially), and the yellow arrows show m. psoas major.

(B and C) Fractional (K_i) (B) and net (K_m) glucose (^{18}FDG) uptake (C) in cervicothoracic tissues during cold exposure.

(D–F) Total glucose uptake (D) and percent plasma glucose turnover (E) taken up by skeletal muscle and BAT. Glucose partitioning from whole-body PET scanning (expressed in SUV) during cold exposure without and with oral ingestion of NiAc (F).

(G) Association between net glucose uptake and shivering intensity in the m. pectoralis major. The data are reported as the mean with 95% CI. Different from BAT at ****$p < 0.0001$, ***$p < 0.001$, **$p < 0.01$, and *$p < 0.05$ and different from control $^{\#}p < 0.05$ and two-way ANOVA with Bonferonni post-hoc test.

can estimate the BAT NEFA uptake to amount to 20 mg over the course of the 3 hr cold exposure when given NiAc, compared to approximately 33 mg in the control condition (Blondin et al., 2015a; Din et al., 2016; Ouellet et al., 2012). Even in the condition where circulating NEFA supply is low, following NiAc ingestion, this would still only represent 0.2% of plasma NEFA turnover. Combined, we believe that a reduction in BAT glucose uptake and circulating NEFA availability played a negligible role in the inhibition of BAT thermogenesis. Some in vitro data suggest that only 50% of NEFA released from the hydrolysis of intracellular TG is oxidized (Mottillo et al., 2016), with the remainder likely re-esterified or released out of the brown adipocyte. Although we show intracellular TG lipolysis to be essential for BAT thermogenesis, direct in vivo quantification of intracellular BAT TG utilization will therefore be required to definitively confirm intracellular TG as the primary fuel for BAT thermogenesis.

Since the first major studies examining the presence of BAT in adult humans were published in 2009 (Cypess et al., 2009; van Marken Lichtenbelt et al., 2009; Virtanen et al., 2009), BAT glucose uptake (^{18}FDG uptake) has been used as an indicator of BAT thermogenesis. In addition to ^{18}FDG, our protocol uses ^{11}C-acetate, a PET tracer that measures BAT oxidative metabolism even in overweight men with and without well-controlled T2D despite remarkably low levels of BAT glucose uptake (Blondin et al., 2015a). In the present study, we show that BAT glucose uptake is associated with cold-induced tissue perfusion ($\rho = 0.60$, $p = 0.02$) and changes in tissue radio-density ($\rho = 0.64$, $p = 0.009$), but not oxidative metabolism ($\rho = 0.21$, $p = 0.44$). We also observed unaltered BAT perfusion and a relatively small reduction in BAT glucose uptake compared to the profound reduction in BAT oxidative metabolism during NiAc administration. The present study provides evidence in humans

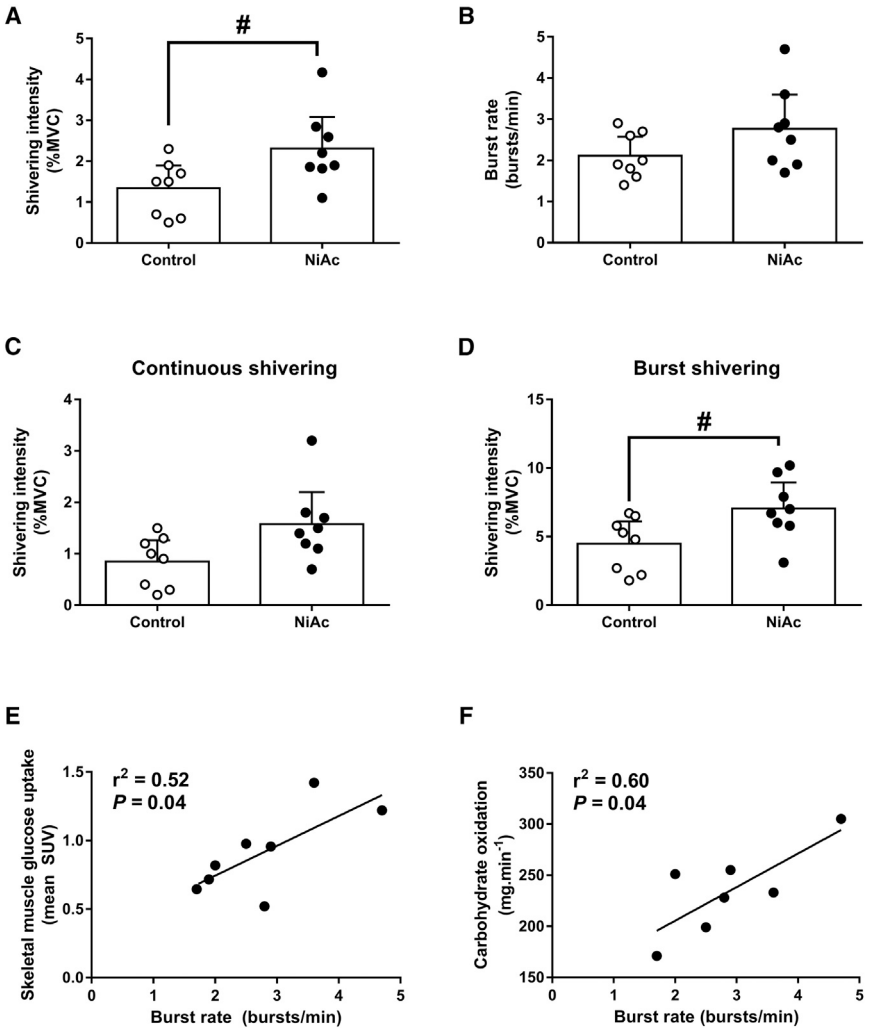

Figure 4. Shivering Response

(A–F) Mean shivering intensity (A) and burst rate (B) of eight muscles during cold exposure without and with oral ingestion of NiAc. The shivering intensity of continuous (C) and burst shivering patterns (D) during cold exposure without and with oral ingestion of NiAc is shown. The relationship between shivering burst rate and skeletal muscle glucose uptake (E) and whole-body carbohydrate oxidation (F) is shown. The data are reported as the mean with 95% CI. Different from control at $^{\#}p < 0.05$ and paired-sample t test.

that a cold-induced increase in BAT perfusion is independent of cold-induced BAT thermogenesis, a concept that has recently been shown in mice (Abreu-Vieira et al., 2015; Ernande et al., 2016). Combined, these findings suggest that, similar to skeletal muscles, an increase in BAT perfusion may be responsible, at least partially, for an increase in BAT glucose uptake, but that glucose uptake is not invariably a reliable marker of BAT thermogenesis. Our results also support the notion that cold-induced increases in BAT radio-density are mainly caused by reduced BAT TG content, not increases in BAT blood flow.

It should be noted that there are experimental settings in which BAT blood flow and BAT glucose uptake may incidentally correlate with BAT thermogenesis and others where there is a complete disassociation. For instance, cold exposure in lean, healthy individuals may result in a sympathetically mediated increase in BAT blood flow, glucose uptake, and thermogenesis, which occur simultaneously. However, cold-stimulated overweight individuals with or without type 2 diabetes have been shown to have impaired BAT blood flow and BAT glucose uptake (Blondin et al., 2015a; Orava et al., 2013), but normal BAT oxidative metabolism (Blondin et al., 2015a), resulting in a disassociation between these three variables. A similar disassociation has been shown upon norepinephrine stimulation in mice lacking uncoupling protein 1 (UCP1), where BAT blood flow still increases, despite an inability to produce heat, while BAT blood flow in these mice also increases in response to a glucose injection (Abreu-Vieira et al., 2015). Others have also shown that insulin stimulation in lean, healthy individuals increases BAT glucose extraction without increasing BAT blood flow (Orava et al., 2011). In the absence of a direct in vivo measure of BAT thermogenesis (e.g., [^{15}O]-oxygen or [^{11}C]-acetate PET), it is difficult to interpret the implication of a difference in blood flow or glucose uptake on BAT thermogenesis.

The near complete inhibition of BAT oxidative metabolism, when given NiAc, was fully compensated by a 149% increase in shivering intensity. Others have also reported an increase in self-perceived shivering when ingesting NiAc during cold exposure, yet, paradoxically, this was also accompanied by a decrease in heat production (Doi et al., 1979). Using electromyography, two distinct shivering patterns emerge, which are associated with the recruitment of specific motor units (Blondin et al., 2014b; Haman et al., 2004a). Under various metabolic conditions, the shivering pattern/muscle fiber recruitment may be modulated to account for the available substrate or thermogenic requirements, without changes in total body heat production (Haman et al., 2004a, 2004c). Here, we show that the shivering pattern was modulated, likely to account for a reduction in WAT lipolysis (Figures 1A and 1B) and possibly intramyocellular hydrolysis of TG, by increasing the frequency and amplitude of burst shivering (Figures 4B and 4D), indicating greater recruitment of high-threshold motor units (type II muscle fibers, fast glycolytic) (Haman et al., 2004b). The differences in burst rate when given NiAc were strongly associated with greater skeletal muscle glucose uptake ($r = 0.72$, $p = 0.01$) and whole-body carbohydrate oxidation ($r = 0.78$, $p = 0.04$). Similarly, the myocardium also showed remarkable metabolic flexibility by also increasing glucose uptake when intracellular hydrolysis of TG was suppressed, as previously shown, at least in part through reduced substrate competition from circulating NEFA

(Knuuti et al., 1994; Vosselman et al., 2012). Despite the NiAc-induced blunting of cold-stimulated BAT oxidative metabolism and increase in cardiac glucose uptake, NiAc did not change whole-body fatty acid oxidation rates. It should be noted that residual Ra_{NEFA} during NiAc administration was enough to provide fatty acids to meet the rate of whole-body fatty acid oxidation even if one assumes complete NiAc-mediated suppression of intracellular TG utilization (Ra_{NEFA} in cold: 222 μmol.min^{-1} [95% CI: 78 to 366]; FA oxidation in cold: 208 μmol.min^{-1} [95% CI: 101 to 316]). It is therefore likely that the utilization of intracellular oxidative substrates likely changed in other organs to maintain total fatty acid oxidation rates.

There was a significant NiAc-induced increase in glucagon level during cold exposure. This result is intriguing and may suggest the need for increased glucagon secretion in the presence of NiAc-induced reduction in circulating NEFA to maintain hepatic glucose output (see Lam et al., 2003 for review). Glucagon at physiological concentrations does not significantly stimulate adipose tissue intracellular lipolysis in vivo in humans (Bertin et al., 2001; Gravholt et al., 2001).

In conclusion, this study provides three critical experimental findings regarding BAT thermogenesis in humans. First, we provide direct experimental evidence supporting the critical role of intracellular TG lipolysis for BAT thermogenesis in humans. Second, we demonstrate that adrenergic stimulation of BAT blood flow is independent of BAT thermogenesis. Accordingly, this shows that both BAT glucose uptake and blood flow are unreliable indicators of BAT thermogenesis. Finally, we also emphasize a reciprocal role of BAT thermogenesis and shivering in cold-induced thermogenesis in humans. This finding supports a physiologically significant thermogenic role of BAT.

EXPERIMENTAL PROCEDURES

Participants took part in two 3-hr cold exposure protocols between November and February (winter), separated by at least 7 days and with the order randomly assigned, in which participants either ingested 150 mg of immediate-release nicotinic acid every 30 min from the onset of cold exposure (50 mg capsules; Galenova), a protocol previously shown to result in a steady suppression of intracellular lipolysis (Carpentier et al., 2005) or a simple cold exposure without nicotinic acid (control). None of the participants were diagnosed with diabetes, based on medical history, repeated assessment of fasting glucose concentration, and 75 g oral glucose tolerance test. None were taking any medication, had any current medical condition known to affect lipid levels or insulin sensitivity, or had known cardiovascular or other medical conditions.

Each acute cold exposure experimental session consisted of a 150 min baseline period at ambient temperature (22.5°C [95% CI: 22.0 to 23.1]), followed by 180 min of cold exposure, elicited using a liquid conditioned suit (Three Piece, Allen-Vanguard) perfused with water at 18°C using a temperature- and flow-controlled circulation bath (Isotemp 6200R28, Fisher Scientific). This protocol was used in order to stimulate low-level shivering and therefore ensuring a cold exposure adequate to evoke BAT stimulation (Blondin et al., 2014a, 2015a, 2015b; Ouellet et al., 2012). Experiments were conducted between 07.30 and 15.00 hr, following a 12 hr fast and 48 hr without strenuous physical activity. Subjects were asked to follow a 2 day standard isocaloric diet based upon a 3 day food record, filled a validated questionnaire for physical activity (Sallis et al., 1985), and underwent portable arm band accelerometry for 7 days (St-Onge et al., 2007). Upon their arrival in the laboratory, subjects wearing only shorts were weighed and instrumented with autonomous wireless temperature sensors (Thermochron iButton model DS1922H, Maxim) placed on 12 sites to measure mean skin temperature (Hardy et al., 1938). Surface electromyography electrodes (Delsys, EMG System) were placed on the belly of eight muscles known to contribute significantly to shivering during cold exposure and monitored continuously (Bell et al., 1992; Blondin et al., 2015b; Haman et al., 2004a, 2005): m. pectoralis major, m. deltoideus, m. trapezius, m. sternocleidomastoid, m. biceps brachii, m. rectus femoris, m. vastus medialis, and m. vastus lateralis. Participants were then fitted with the liquid-conditioned suit, swallowed a telemetric thermometry capsule to measure core temperature (VitalSense monitor and Jonah temperature capsule, Mini-Mitter), and performed a series of maximal voluntary contractions (MVC) for each of the eight muscles being recorded by sEMG for normalization of the shivering measures. Shivering intensity and shivering pattern were determined as previously described (Blondin et al., 2015b; Haman et al., 2004a, 2004b, 2005). In brief, shivering intensity of individual muscles was determined from root-mean-square (RMS) values calculated from raw EMG, normalized to MVC RMS, and corrected for baseline RMS (Haman et al., 2004a, 2004b). Shivering pattern is based on the identification of two distinct patterns of shivering: (1) continuous, low-intensity shivering and (2) bursts of high-intensity shivering (see Haman et al., 2004a for full procedure for shivering burst identification). These patterns are distinguished according to differences in frequency of occurrence (4–8 Hz for continuous versus 0.1–0.2 Hz for bursts) and intensity (2.5% MVC for continuous versus 7%–15% MVC for bursts) (Haman et al., 2004a; Israel and Pozos, 1989). Upon completing a series of muscle contractions, indwelling catheters were then placed in an antecubital vein in both arms for blood sampling and tracer infusions. Participants were asked to empty their bladder and a primed continuous infusion of [3-^{3}H]-glucose to measure $Ra_{glucose}$ (Carpentier et al., 2001), [U-^{13}C]-palmitate to measure Ra_{NEFA}, and [1,1,2,3,3-^{2}H]-glycerol to measure $Ra_{glycerol}$ (Carpentier et al., 2005) were started (time = 0 min). Only the sampling times 130, 140, 150, 280, 290, and 300 min were used to calculate steady-state $Ra_{glucose}$, Ra_{NEFA}, and $Ra_{glycerol}$. Whole-body shivering intensity and pattern as well as mean skin and core temperatures were measured continuously from time 120 to 300 min as previously described (Haman et al., 2004b). Whole-body metabolic heat production was determined by indirect respiratory calorimetry, corrected for protein oxidation (Haman et al., 2002) at room temperature and between times 180 to 200 min and 280 to 300 min (i.e., 60 to 80 min and 160 to 180 min after the beginning of cold exposure). Fatty acid oxidation (in μmol.min^{-1}) was calculated from triglyceride oxidation (in g.min^{-1}) assuming the average molecular weight of triglyceride as 861 g.mol^{-1} and multiplying the molar rate of triglyceride oxidation by three to account for each mole of triglyceride containing three moles of fatty acids (Frayn, 1983; Hirsch, 2010).

PET and CT Protocol

Participants remained supine in a PET and CT scanner (Philips Gemini GXL; Philips) for 120 min at ambient temperature and throughout the duration of the 180 min cold exposure. Tissue-specific oxidative metabolism was determined by first performing a CT scan (40 mAs) centered at the cervico-thoracic junction to correct for attenuation and to define PET regions of interest (ROI). At time 90 min (room temperature) and at time 210 min (i.e., 90 min after onset of cold exposure) a ~185 MBq i.v. bolus of ^{11}C-acetate was injected intravenously and was followed by a 30 min list-mode dynamic PET acquisition centered at the cervico-thoracic junction (Ouellet et al., 2012). Tissue oxidative metabolism index (the rapid fractional tissue clearance of ^{11}C-acetate, k, in s^{-1}) was estimated from tissue ^{11}C activity over time using monoexponential fit from the time of peak tissue activity (Buck et al., 1991). Tissue-specific glucose uptake was determined by injecting an ~185 MBq i.v. bolus of [^{18}F]-FDG at time 240 (i.e., 120 min after onset of cold exposure), followed by a dynamic PET acquisition centered at the cervicothoracic junction. The CT performed prior to the ^{11}C-acetate injection in the cold was used to correct for attenuation and to define PET ROI for the [^{18}F]-FDG scans. Further, any residual ^{11}C-acetate activity prior to [^{18}F]-FDG scans are corrected by acquiring a 120 s frame prior to the injection of [^{18}F]-FDG and accounting for the disintegration rate of ^{11}C. Plasma and tissue time-radioactivity curves for ^{18}FDG were analyzed graphically using the Patlak linearization method (Ménard et al., 2010; Patlak et al., 1983), with the image-derived arterial input function taken from the aortic arch (Croteau et al., 2010). The slope of the plot in the graphical analysis is equal to glucose fractional uptake (K_i in min^{-1}). Net glucose uptake (K_m) was then calculated by multiplying K_i by plasma glucose

concentration, measured during the PET imaging protocol, which assumes a lump constant value of 1.0 compared with endogenous plasma glucose. Following cold exposure, a whole-body CT scan (16 mAs) and whole-body static PET acquisition were performed to determine whole-body ^{18}FDG organ distribution and tissue standard uptake value (SUV).

PET and CT Image Analyses

ROI were first defined from the transaxial CT slices, then copied to ^{11}C-acetate, and then to ^{18}FDG PET image sequences. For dynamic PET acquisitions, mean value of pixels (mean SUV) for each frame was recorded. ROI were drawn on the aortic arch for blood activity (input functions), the larger skeletal muscles in the field of view (e.g., m. sternocleidomastoid, m. trapezius, m. pectoralis major, and m. deltoideus), on posterior cervical subcutaneous adipose tissue and on supraclavicular BAT. For whole-body scans, ROI were first defined from the transaxial CT slices and then co-registered to ^{18}FDG image sequences. Mean values of pixels (mean SUV) of ROI were determined for the myocardium, liver, abdominal subcutaneous white adipose tissue (scWAT), peri-renal white adipose tissue (vWAT), and bilaterally for BAT, and the following muscles: m. sternocleidomastoid, m. longus colli, m. trapezius, m. lattissimus dorsi, m. pectoralis major, m. deltoideus, m. biceps brachii, m. triceps brachii, m.brachioradialis, m. erector spinae, m.rectus abdominis, m. psoas major, m. adductor magnus, m. gluteus maximus, m. biceps femoris, m. rectus femoris, m. vastus medialis, m. vastus lateralis.

Biological Assays

Plasma glucose, insulin, total NEFA, and TG were measured as previously described (Carpentier et al., 2005). Plasma cortisol, TSH, free T3, and free T4 were measured using specific electrochemiluminescent immunoassays (Ouellet et al., 2012). Individual plasma NEFA (palmitate, linoleate, and oleate), glycerol, and [U-^{13}C]-palmitate enrichment and [1,1,2,3,3-^{2}H]-glycerol enrichment were measured by gas chromatography-mass spectrometry (Carpentier et al., 2005). [3-^{3}H]-glucose specific activity was determined by liquid scintillation spectrometry, as described (Carpentier et al., 2001).

Statistical Analysis

Data are expressed as mean with 95% CI. Paired Student's t test was used to compare between acute cold exposure experimental sessions. Two-way ANOVA for repeated-measures was used to analyze NiAc- and temperature-dependent differences in averaged steady-state hormone and metabolite levels and blood and tissue PET-acquired activities throughout the protocols. Bonferonni's multiple comparisons post-hoc test was used, where applicable. Appropriate transformations of variables were performed when normal distribution was not observed for parametric statistical testing. Pearson correlation coefficients were used to determine correlation between variables. A two-tailed p value of less than 0.05 was considered significant. The n = 8 participants were chosen on the assumption of complete NiAc-mediated blunting of cold-stimulated BAT oxidative metabolism. Using previously published data in healthy men (Blondin et al., 2014a; Ouellet et al., 2012), we determined that n = 8 participants would result in >85% power to detect such a within subject difference, at an alpha level of 0.05. All analyses were performed using SPSS for Windows (version 21.0; SPSS) or GraphPad Prism version 6.0 for Windows (GraphPad).

Study Approval

Informed written consent was obtained from all participants in accordance with the Declaration of Helsinki, and the protocol received approval from the Human Ethics Committee of the Centre de Recherche du Centre hospitalier universitaire de Sherbrooke.

AUTHOR CONTRIBUTIONS

Conception and design of the experiments: A.C.C., D.P.B., F.H., D.R., and E.E.T. Collection, analysis, and interpretation of data: D.P.B., F.F., S.P., F.H., E.E.T., D.R., and A.C.C. Drafting the article or revising it critically for important intellectual content: D.P.B., F.F., S.P., B.G., E.E.T., D.R., F.H., and A.C.C.

ACKNOWLEDGMENTS

The authors would like to acknowledge the excellent technical assistance provided by Diane Lessard, Caroll-Lynn Thibodeau, Maude Gérard, Éric Lavallée, Lucie Bouffard, and Mélanie Fortin. This work was supported by a grant from the Canadian Institutes of Health Research (CIHR) to A.C.C. and from the Natural Sciences and Engineering Research Council of Canada (NSERC) to F.H. D.P.B. is a recipient of a CIHR Post-doctoral fellowship. A.C.C. is the recipient of the CIHR-GlaxoSmithKline Chair in Diabetes. D.R. is the recipient of the CIHR/Merck Frosst Research Chair on Obesity. The Centre de Recherche du Centre Hospitalier Universitaire de Sherbrooke is funded by the Fonds de Recherche du Québec - Santé.

Received: July 26, 2016
Revised: October 21, 2016
Accepted: December 10, 2016
Published: January 12, 2017

REFERENCES

Abreu-Vieira, G., Hagberg, C.E., Spalding, K.L., Cannon, B., and Nedergaard, J. (2015). Adrenergically stimulated blood flow in brown adipose tissue is not dependent on thermogenesis. Am. J. Physiol. Endocrinol. Metab. *308*, E822–E829.

Ahmed, K., Tunaru, S., and Offermanns, S. (2009). GPR109A, GPR109B and GPR81, a family of hydroxy-carboxylic acid receptors. Trends Pharmacol. Sci. *30*, 557–562.

Baba, S., Jacene, H.A., Engles, J.M., Honda, H., and Wahl, R.L. (2010). CT Hounsfield units of brown adipose tissue increase with activation: preclinical and clinical studies. J. Nucl. Med. *51*, 246–250.

Barquissau, V., Beuzelin, D., Pisani, D.F., Beranger, G.E., Mairal, A., Montagner, A., Roussel, B., Tavernier, G., Marques, M.A., Moro, C., et al. (2016). White-to-brite conversion in human adipocytes promotes metabolic reprogramming towards fatty acid anabolic and catabolic pathways. Mol. Metab. *5*, 352–365.

Bartness, T.J., Liu, Y., Shrestha, Y.B., and Ryu, V. (2014). Neural innervation of white adipose tissue and the control of lipolysis. Front. Neuroendocrinol. *35*, 473–493.

Bell, D.G., Tikuisis, P., and Jacobs, I. (1992). Relative intensity of muscular contraction during shivering. J. Appl. Physiol. *72*, 2336–2342.

Bertin, E., Arner, P., Bolinder, J., and Hagström-Toft, E. (2001). Action of glucagon and glucagon-like peptide-1-(7-36) amide on lipolysis in human subcutaneous adipose tissue and skeletal muscle in vivo. J. Clin. Endocrinol. Metab. *86*, 1229–1234.

Blondin, D.P., Labbé, S.M., Tingelstad, H.C., Noll, C., Kunach, M., Phoenix, S., Guérin, B., Turcotte, É.E., Carpentier, A.C., Richard, D., and Haman, F. (2014a). Increased brown adipose tissue oxidative capacity in cold-acclimated humans. J. Clin. Endocrinol. Metab. *99*, E438–E446.

Blondin, D.P., Tingelstad, H.C.L., Mantha, O., Gosselin, C., and Haman, F. (2014b). Maintaining thermogenesis in cold exposed humans: relying on multiple metabolic pathways. In Comprehensive Physiology (John Wiley & Sons, Inc.), pp. 1383–1402.

Blondin, D.P., Labbé, S.M., Noll, C., Kunach, M., Phoenix, S., Guérin, B., Turcotte, E.E., Haman, F., Richard, D., and Carpentier, A.C. (2015a). Selective impairment of glucose but not fatty acid or oxidative metabolism in brown adipose tissue of subjects with type 2 diabetes. Diabetes *64*, 2388–2397.

Blondin, D.P., Labbé, S.M., Phoenix, S., Guérin, B., Turcotte, E.E., Richard, D., Carpentier, A.C., and Haman, F. (2015b). Contributions of white and brown adipose tissues and skeletal muscles to acute cold-induced metabolic responses in healthy men. J. Physiol. *593*, 701–714.

Brito, M.N., Brito, N.A., Brito, S.R., Moura, M.A., Kawashita, N.H., Kettelhut, I.C., and Migliorini, R.H. (1999). Brown adipose tissue triacylglycerol synthesis in rats adapted to a high-protein, carbohydrate-free diet. Am. J. Physiol. *276*, R1003–R1009.

Buck, A., Wolpers, H.G., Hutchins, G.D., Savas, V., Mangner, T.J., Nguyen, N., and Schwaiger, M. (1991). Effect of carbon-11-acetate recirculation on estimates of myocardial oxygen consumption by PET. J. Nucl. Med. *32*, 1950–1957.

Cannon, B., and Nedergaard, J. (2004). Brown adipose tissue: function and physiological significance. Physiol. Rev. *84*, 277–359.

Carpentier, A., Patterson, B.W., Uffelman, K.D., Giacca, A., Vranic, M., Cattral, M.S., and Lewis, G.F. (2001). The effect of systemic versus portal insulin delivery in pancreas transplantation on insulin action and VLDL metabolism. Diabetes *50*, 1402–1413.

Carpentier, A.C., Frisch, F., Cyr, D., Généreux, P., Patterson, B.W., Giguère, R., and Baillargeon, J.P. (2005). On the suppression of plasma nonesterified fatty acids by insulin during enhanced intravascular lipolysis in humans. Am. J. Physiol. Endocrinol. Metab. *289*, E849–E856.

Croteau, E., Lavallée, E., Labbe, S.M., Hubert, L., Pifferi, F., Rousseau, J.A., Cunnane, S.C., Carpentier, A.C., Lecomte, R., and Bénard, F. (2010). Image-derived input function in dynamic human PET/CT: methodology and validation with 11C-acetate and 18F-fluorothioheptadecanoic acid in muscle and 18F-fluorodeoxyglucose in brain. Eur. J. Nucl. Med. Mol. Imaging *37*, 1539–1550.

Cypess, A.M., Lehman, S., Williams, G., Tal, I., Rodman, D., Goldfine, A.B., Kuo, F.C., Palmer, E.L., Tseng, Y.H., Doria, A., et al. (2009). Identification and importance of brown adipose tissue in adult humans. N. Engl. J. Med. *360*, 1509–1517.

Cypess, A.M., Chen, Y.C., Sze, C., Wang, K., English, J., Chan, O., Holman, A.R., Tal, I., Palmer, M.R., Kolodny, G.M., and Kahn, C.R. (2012). Cold but not sympathomimetics activates human brown adipose tissue in vivo. Proc. Natl. Acad. Sci. USA *109*, 10001–10005.

Din, M.U., Raiko, J., Saari, T., Kudomi, N., Tolvanen, T., Oikonen, V., Teuho, J., Sipila, H.T., Savisto, N., Parkkola, R., et al. (2016). Human brown adipose tissue [O]O PET imaging in the presence and absence of cold stimulus. Eur. J. Nucl. Med. Mol. Imaging *43*, 1878–1886.

Doi, K., Ohno, T., Kurahashi, M., and Kuroshima, A. (1979). Thermoregulatory nonshivering thermogenesis in men, with special reference to lipid metabolism. Jpn. J. Physiol. *29*, 359–372.

Ernande, L., Stanford, K.I., Thoonen, R., Zhang, H., Clerte, M., Hirshman, M.F., Goodyear, L.J., Bloch, K.D., Buys, E.S., and Scherrer-Crosbie, M. (2016). Relationship of brown adipose tissue perfusion and function: a study through beta2-adrenoreceptor stimulation. J. Appl. Physiol. (1985) *120*, 825–832.

Fedorenko, A., Lishko, P.V., and Kirichok, Y. (2012). Mechanism of fatty-acid-dependent UCP1 uncoupling in brown fat mitochondria. Cell *151*, 400–413.

Frayn, K.N. (1983). Calculation of substrate oxidation rates in vivo from gaseous exchange. J. Appl. Physiol. *55*, 628–634.

Gravholt, C.H., Møller, N., Jensen, M.D., Christiansen, J.S., and Schmitz, O. (2001). Physiological levels of glucagon do not influence lipolysis in abdominal adipose tissue as assessed by microdialysis. J. Clin. Endocrinol. Metab. *86*, 2085–2089.

Haemmerle, G., Lass, A., Zimmermann, R., Gorkiewicz, G., Meyer, C., Rozman, J., Heldmaier, G., Maier, R., Theussl, C., Eder, S., et al. (2006). Defective lipolysis and altered energy metabolism in mice lacking adipose triglyceride lipase. Science *312*, 734–737.

Haman, F., Péronnet, F., Kenny, G.P., Massicotte, D., Lavoie, C., Scott, C., and Weber, J.-M. (2002). Effect of cold exposure on fuel utilization in humans: plasma glucose, muscle glycogen, and lipids. J. Appl. Physiol. *93*, 77–84.

Haman, F., Legault, S.R., Rakobowchuk, M., Ducharme, M.B., and Weber, J.-M. (2004a). Effects of carbohydrate availability on sustained shivering II. Relating muscle recruitment to fuel selection. J. Appl. Physiol. *96*, 41–49.

Haman, F., Legault, S.R., and Weber, J.-M. (2004b). Fuel selection during intense shivering in humans: EMG pattern reflects carbohydrate oxidation. J. Physiol. *556*, 305–313.

Haman, F., Péronnet, F., Kenny, G.P., Doucet, E., Massicotte, D., Lavoie, C., and Weber, J.-M. (2004c). Effects of carbohydrate availability on sustained shivering I. Oxidation of plasma glucose, muscle glycogen, and proteins. J. Appl. Physiol. *96*, 32–40.

Haman, F., Péronnet, F., Kenny, G.P., Massicotte, D., Lavoie, C., and Weber, J.-M. (2005). Partitioning oxidative fuels during cold exposure in humans: muscle glycogen becomes dominant as shivering intensifies. J. Physiol. *566*, 247–256.

Hanssen, M.J., Hoeks, J., Brans, B., van der Lans, A.A., Schaart, G., van den Driessche, J.J., Jörgensen, J.A., Boekschoten, M.V., Hesselink, M.K., Havekes, B., et al. (2015). Short-term cold acclimation improves insulin sensitivity in patients with type 2 diabetes mellitus. Nat. Med. *21*, 863–865.

Hardy, J.D., Du Bois, E.F., and Soderstrom, G.F. (1938). The technic of measuring radiation and convection: one figure. J. Nutr. *15*, 461–475.

Himms-Hagen, J. (1965). Lipid metabolism in warm-acclimated and cold-acclimated rats exposed to cold. Can. J. Physiol. Pharmacol. *43*, 379–403.

Hirsch, J. (2010). Fatty acid patterns in human adipose tissue. In Comprehensive Physiology (John Wiley & Sons, Inc.). Published online January 1, 2011. http://dx.doi.org/10.1002/cphy.cp050117.

Horowitz, J.F., Coppack, S.W., Paramore, D., Cryer, P.E., Zhao, G., and Klein, S. (1999). Effect of short-term fasting on lipid kinetics in lean and obese women. Am. J. Physiol. *276*, E278–E284.

Israel, D.J., and Pozos, R.S. (1989). Synchronized slow-amplitude modulations in the electromyograms of shivering muscles. J. Appl. Physiol. *66*, 2358–2363.

Jocken, J.W., Langin, D., Smit, E., Saris, W.H., Valle, C., Hul, G.B., Holm, C., Arner, P., and Blaak, E.E. (2007). Adipose triglyceride lipase and hormone-sensitive lipase protein expression is decreased in the obese insulin-resistant state. J. Clin. Endocrinol. Metab. *92*, 2292–2299.

Jocken, J.W., Goossens, G.H., van Hees, A.M., Frayn, K.N., van Baak, M., Stegen, J., Pakbiers, M.T., Saris, W.H., and Blaak, E.E. (2008). Effect of beta-adrenergic stimulation on whole-body and abdominal subcutaneous adipose tissue lipolysis in lean and obese men. Diabetologia *51*, 320–327.

Knuuti, M.J., Yki-Järvinen, H., Voipio-Pulkki, L.M., Mäki, M., Ruotsalainen, U., Härkönen, R., Teräs, M., Haaparanta, M., Bergman, J., Hartiala, J., et al. (1994). Enhancement of myocardial [fluorine-18]fluorodeoxyglucose uptake by a nicotinic acid derivative. J. Nucl. Med. *35*, 989–998.

Labbé, S.M., Caron, A., Bakan, I., Laplante, M., Carpentier, A.C., Lecomte, R., and Richard, D. (2015). In vivo measurement of energy substrate contribution to cold-induced brown adipose tissue thermogenesis. FASEB J. *29*, 2046–2058.

Lam, T.K., Carpentier, A., Lewis, G.F., van de Werve, G., Fantus, I.G., and Giacca, A. (2003). Mechanisms of the free fatty acid-induced increase in hepatic glucose production. Am. J. Physiol. Endocrinol. Metab. *284*, E863–E873.

Laplante, M., Festuccia, W.T., Soucy, G., Blanchard, P.G., Renaud, A., Berger, J.P., Olivecrona, G., and Deshaies, Y. (2009). Tissue-specific postprandial clearance is the major determinant of PPARgamma-induced triglyceride lowering in the rat. Am. J. Physiol. Regul. Integr. Comp. Physiol. *296*, R57–R66.

Lee, J., Ellis, J.M., and Wolfgang, M.J. (2015). Adipose fatty acid oxidation is required for thermogenesis and potentiates oxidative stress-induced inflammation. Cell Rep. *10*, 266–279.

Li, Y., Fromme, T., Schweizer, S., Schöttl, T., and Klingenspor, M. (2014). Taking control over intracellular fatty acid levels is essential for the analysis of thermogenic function in cultured primary brown and brite/beige adipocytes. EMBO Rep. *15*, 1069–1076.

Ménard, S.L., Croteau, E., Sarrhini, O., Gélinas, R., Brassard, P., Ouellet, R., Bentourkia, M., van Lier, J.E., Des Rosiers, C., Lecomte, R., and Carpentier, A.C. (2010). Abnormal in vivo myocardial energy substrate uptake in diet-induced type 2 diabetic cardiomyopathy in rats. Am. J. Physiol. Endocrinol. Metab. *298*, E1049–E1057.

Morrison, S.F. (2016). Central neural control of thermoregulation and brown adipose tissue. Auton. Neurosci. *196*, 14–24.

Mottillo, E.P., Desjardins, E.M., Crane, J.D., Smith, B.K., Green, A.E., Ducommun, S., Henriksen, T.I., Rebalka, I.A., Razi, A., Sakamoto, K., et al. (2016). Lack of adipocyte AMPK exacerbates insulin resistance and hepatic steatosis through brown and beige adipose tissue function. Cell Metab. *24*, 118–129.

Moura, M.A., Festuccia, W.T., Kawashita, N.H., Garófalo, M.A., Brito, S.R., Kettelhut, I.C., and Migliorini, R.H. (2005). Brown adipose tissue glyceroneogenesis is activated in rats exposed to cold. Pflugers Arch. *449*, 463–469.

Muzik, O., Mangner, T.J., and Granneman, J.G. (2012). Assessment of oxidative metabolism in brown fat using PET imaging. Front. Endocrinol. (Lausanne) *3*, 15.

Muzik, O., Mangner, T.J., Leonard, W.R., Kumar, A., Janisse, J., and Granneman, J.G. (2013). 15O PET measurement of blood flow and oxygen consumption in cold-activated human brown fat. J. Nucl. Med. *54*, 523–531.

Olsen, J.M., Sato, M., Dallner, O.S., Sandström, A.L., Pisani, D.F., Chambard, J.C., Amri, E.Z., Hutchinson, D.S., and Bengtsson, T. (2014). Glucose uptake in brown fat cells is dependent on mTOR complex 2-promoted GLUT1 translocation. J. Cell Biol. *207*, 365–374.

Orava, J., Nuutila, P., Lidell, M.E., Oikonen, V., Noponen, T., Viljanen, T., Scheinin, M., Taittonen, M., Niemi, T., Enerbäck, S., and Virtanen, K.A. (2011). Different metabolic responses of human brown adipose tissue to activation by cold and insulin. Cell Metab. *14*, 272–279.

Orava, J., Nuutila, P., Noponen, T., Parkkola, R., Viljanen, T., Enerbäck, S., Rissanen, A., Pietiläinen, K.H., and Virtanen, K.A. (2013). Blunted metabolic responses to cold and insulin stimulation in brown adipose tissue of obese humans. Obesity (Silver Spring) *21*, 2279–2287.

Osuga, J., Ishibashi, S., Oka, T., Yagyu, H., Tozawa, R., Fujimoto, A., Shionoiri, F., Yahagi, N., Kraemer, F.B., Tsutsumi, O., and Yamada, N. (2000). Targeted disruption of hormone-sensitive lipase results in male sterility and adipocyte hypertrophy, but not in obesity. Proc. Natl. Acad. Sci. USA *97*, 787–792.

Ouellet, V., Labbé, S.M., Blondin, D.P., Phoenix, S., Guérin, B., Haman, F., Turcotte, E.E., Richard, D., and Carpentier, A.C. (2012). Brown adipose tissue oxidative metabolism contributes to energy expenditure during acute cold exposure in humans. J. Clin. Invest. *122*, 545–552.

Patlak, C.S., Blasberg, R.G., and Fenstermacher, J.D. (1983). Graphical evaluation of blood-to-brain transfer constants from multiple-time uptake data. J. Cereb. Blood Flow Metab. *3*, 1–7.

Sallis, J.F., Haskell, W.L., Wood, P.D., Fortmann, S.P., Rogers, T., Blair, S.N., and Paffenbarger, R.S.J., Jr. (1985). Physical activity assessment methodology in the Five-City Project. Am. J. Epidemiol. *121*, 91–106.

St-Onge, M., Mignault, D., Allison, D.B., and Rabasa-Lhoret, R. (2007). Evaluation of a portable device to measure daily energy expenditure in free-living adults. Am. J. Clin. Nutr. *85*, 742–749.

Tadamura, E., Tamaki, N., Matsumori, A., Magata, Y., Yonekura, Y., Nohara, R., Sasayama, S., Yoshibayashi, M., Kamiya, T., and Konishi, J. (1996). Myocardial metabolic changes in hypertrophic cardiomyopathy. J. Nucl. Med. *37*, 572–577.

van Marken Lichtenbelt, W.D., Vanhommerig, J.W., Smulders, N.M., Drossaerts, J.M., Kemerink, G.J., Bouvy, N.D., Schrauwen, P., and Teule, G.J. (2009). Cold-activated brown adipose tissue in healthy men. N. Engl. J. Med. *360*, 1500–1508.

Virtanen, K.A., Lidell, M.E., Orava, J., Heglind, M., Westergren, R., Niemi, T., Taittonen, M., Laine, J., Savisto, N.J., Enerbäck, S., and Nuutila, P. (2009). Functional brown adipose tissue in healthy adults. N. Engl. J. Med. *360*, 1518–1525.

Vosselman, M.J., van der Lans, A.A., Brans, B., Wierts, R., van Baak, M.A., Schrauwen, P., and van Marken Lichtenbelt, W.D. (2012). Systemic β-adrenergic stimulation of thermogenesis is not accompanied by brown adipose tissue activity in humans. Diabetes *61*, 3106–3113.